

Supporting information

Table S1. The prediction of binding site on HIV-1 integrase.

Binding Site	Residues	Docking Score
S1	D64, D116, N117, G118, F121, Y143, N144, P145, Q148, E152.	-7.269
S2	W61, T97, A98, L101, L102, A105, P109, F121, A129, C130, W132, A133, I135.	-3.346
S3	E48, A49, M50, H51, Q216, I217, T218, K219, I220, Q221, N222, V225, L241, K244, G245, E246, A248, V249, R262, A265, K266, I267.	-5.954
S4	D55, C56, Q53, I60, W61, Q62, V77, V79, S81, H114, G138, Q146, S147, V150, R187, G192, A196, R199, I203, I204, A205, I208, T210, K211.	-5.459
S5	A38, D41, C43, Q44, L45, K46, G47, E48, Y226, D229, R231, P233, W235, G237, P238, K266, I267, R269.	-4.555
S6	G47, E48, A49, M50, T235, R262, R263, A265, K266.	-3.711
S7	I84, E85, A86, E87, A88, K103, R107, K173, V176, Q177, V180.	-4.553

Table S2. The detail energy components contribution of calculated binding free energies of studied inhibitors JMC6F, DTG and MK1 binding to HIV-1 IN and RNase H.

Systems	$\Delta E_{\text{ele}}^{\text{a}}$	$\Delta E_{\text{vdw}}^{\text{b}}$	$\Delta G_{\text{pol,PB}}^{\text{c}}$	$\Delta G_{\text{nonpol,PB}}^{\text{d}}$	$\Delta G_{\text{total,PB}}^{\text{e}}$
IN-JMC6F	-78.21 \pm 0.45	-25.18 \pm 0.17	86.32 \pm 0.33	-4.83 \pm 0.01	-21.89 \pm 0.27
RNase H-JMC6F	-57.80 \pm 0.25	-37.14 \pm 0.16	83.06 \pm 0.25	-5.42 \pm 0.08	-17.30 \pm 0.22
RNase H-MK1	-60.62 \pm 0.47	-17.73 \pm 0.19	64.37 \pm 0.30	-3.54 \pm 0.08	-17.50 \pm 0.30
IN-DTG	-82.87 \pm 0.26	-35.67 \pm 0.16	90.95 \pm 0.21	-5.24 \pm 0.06	-32.83 \pm 0.19
IN-EVG	-66.43 \pm 0.32	-44.64 \pm 0.20	88.40 \pm 0.33	-4.97 \pm 0.04	-28.27 \pm 0.21
IN-RAL	-66.26 \pm 0.23	-51.28 \pm 0.12	51.28 \pm 0.26	-6.03 \pm 0.02	-31.34 \pm 0.17

All units are kcal/mol.

^a Electrostatic energy.

^b Van der Waals contribution.

^c Solvation free energy.

^d Nonpolar solvation contribution.

^e Total binding free energy.

Table S3. The calculated and estimated binding free energies based on experimental results of RAL, EVG and DTG with HIV-1 IN.

Mutation	RAL				EVG				DTG			
	$\Delta\Delta G_{calc}^a$	FC _{calc} ^b	FC _{exp} ^c	$\Delta\Delta G_{exp}^d$	$\Delta\Delta G_{calc}$	FC _{calc}	FC _{exp}	$\Delta\Delta G_{exp}$	$\Delta\Delta G_{calc}$	FC _{calc}	FC _{exp}	$\Delta\Delta G_{exp}$
T66A	0.40	1.95	0.61	-0.29	1.01	5.50	4.10	0.84	0.30	1.66	0.26	-0.79
T66I	0.50	2.32	0.51	-0.40	1.02	5.59	8.00	1.23	0.10	1.18	0.26	-0.80
T66K	1.52	12.94	9.60	1.34	3.98	824.52	84.00	2.63	0.86	4.27	2.30	0.49
E92Q	1.85	22.65	3.50	0.74	2.90	133.31	36.00	2.12	0.01	1.02	1.60	0.28
E138A	-0.06	0.90	1.00	0.00	0.12	1.22	1.00	0.00	0.01	1.02	1.00	0.00
E138K	0.07	1.13	1.00	0.00	0.98	5.22	1.00	0.00	0.80	3.86	0.90	-0.04
G140C	0.01	1.02	1.00	0.00	-0.14	0.79	1.00	0.00	0.08	1.14	1.00	0.00
G140S	0.32	1.72	1.10	0.06	0.13	1.25	2.70	0.59	0.65	2.99	0.86	-0.09
Y143C	1.01	5.47	3.20	0.69	0.89	4.49	1.50	0.24	0.33	1.75	0.95	-0.03
Y143H	0.98	5.21	1.80	0.35	0.56	2.57	1.50	0.24	0.41	2.00	0.89	-0.07
Y143R	2.32	49.90	16.00	1.64	1.02	5.59	1.80	0.35	1.30	8.96	1.40	0.20
S147G	0.88	4.39	1.10	0.06	1.21	7.70	4.00	0.82	0.39	1.93	1.00	0.00
Q148H	1.34	9.58	13.00	1.52	1.98	28.23	7.30	1.18	0.06	1.11	1.00	0.00
Q148K	5.54	>1700	87.00	2.65	6.02	>1700	1700	4.41	0.30	1.66	1.10	0.06
Q148R	3.02	164.02	47.00	2.28	5.85	>1700	240	3.25	0.25	1.52	1.20	0.11
N155H	2.31	29.96	8.40	1.26	2.53	71.41	25.00	1.91	0.40	1.96	0.99	0.01

^a Calculated binding free energy by MM/PBSA method in this work. All units are kcal/mol.

^b Fold change of potency were derived from by the equation $\Delta\Delta G_{calc} = RT \ln (FC_{potency})$

^c Fold-changes of potency measured by Ki values ($FC_{potency} = EC50_{mutation}/EC50_{wild\ type}$).

^d $\Delta\Delta G_{exp}$ were derived from the $FC_{potency}$ by the equation $\Delta\Delta G_{exp} = RT \ln (FC_{potency})$.

Table S4. The detail energy components contribution of calculated binding free energies of RAL binding to mutated HIV-1 IN

Mutations	ΔE_{ele}	ΔE_{vdw}	$\Delta G_{\text{pol,PB}}$	$\Delta G_{\text{nonpol,PB}}$	$\Delta G_{\text{total,PB}}$
WT	-66.26 ± 0.51	-51.28 ± 0.16	92.23 ± 0.35	-6.03 ± 0.01	-31.34 ± 0.14
T66A	-62.35 ± 0.48	-47.01 ± 0.18	84.01 ± 0.32	-5.58 ± 0.01	-30.94 ± 0.26
T66I	-70.02 ± 0.50	-41.02 ± 0.18	85.4 ± 0.28	-5.21 ± 0.01	-30.84 ± 0.21
T66K	-69.22 ± 0.39	-45.11 ± 0.13	91.31 ± 0.26	-6.47 ± 0.02	-29.82 ± 0.19
E92Q	-59.21 ± 0.44	-53.22 ± 0.17	88.27 ± 0.31	-5.33 ± 0.01	-29.49 ± 0.22
E138A	-67.92 ± 0.53	-36.06 ± 0.19	77.67 ± 0.30	-5.09 ± 0.03	-31.40 ± 0.35
E138K	-75.35 ± 0.47	-33.95 ± 0.16	83.24 ± 0.25	-5.34 ± 0.01	-31.40 ± 0.23
G140C	-66.49 ± 0.38	-35.26 ± 0.15	75.73 ± 0.38	-5.31 ± 0.02	-31.33 ± 0.17
G140S	-76.57 ± 0.37	-36.53 ± 0.14	76.04 ± 0.32	-5.21 ± 0.01	-31.02 ± 0.18
Y143C	-63.06 ± 0.46	-39.08 ± 0.17	77.25 ± 0.30	-5.44 ± 0.00	-30.33 ± 0.15
Y143H	-55.99 ± 0.52	-68.36 ± 0.14	98.98 ± 0.31	-4.99 ± 0.01	-30.36 ± 0.20
Y143R	-74.75 ± 0.43	-33.91 ± 0.15	84.94 ± 0.24	-5.30 ± 0.01	-29.02 ± 0.21
S147G	-69.81 ± 0.43	-49.18 ± 0.16	93.75 ± 0.27	-5.22 ± 0.00	-30.46 ± 0.19
Q148H	-81.67 ± 0.47	-34.57 ± 0.17	91.35 ± 0.26	-5.11 ± 0.02	-30.00 ± 0.14
Q148K	-52.92 ± 0.44	-65.06 ± 0.17	97.23 ± 0.30	-5.05 ± 0.01	-25.80 ± 0.23
Q148R	-75.92 ± 0.49	-38.06 ± 0.16	90.71 ± 0.26	-5.05 ± 0.01	-28.32 ± 0.26
N155H	-79.71 ± 0.52	-32.43 ± 0.15	88.52 ± 0.34	-5.41 ± 0.01	-29.03 ± 0.17

All units are kcal/mol.

Table S5. The detail energy components contribution of calculated binding free energies of EVG binding to mutated HIV-1 IN.

Mutations	ΔE_{ele}	ΔE_{vdw}	$\Delta G_{\text{pol,PB}}$	$\Delta G_{\text{nonpol,PB}}$	$\Delta G_{\text{total,PB}}$
WT	-66.43 \pm 0.37	-44.64 \pm 0.17	88.40 \pm 0.52	-5.55 \pm 0.07	-28.22 \pm 0.45
T66A	-72.35 \pm 0.27	-31.01 \pm 0.20	82.73 \pm 0.28	-5.58 \pm 0.03	-27.21 \pm 0.31
T66I	-62.35 \pm 0.35	-41.01 \pm 0.19	81.74 \pm 0.25	-5.58 \pm 0.05	-27.20 \pm 0.27
T66K	-81.39 \pm 0.28	-29.11 \pm 0.25	91.46 \pm 0.32	-5.20 \pm 0.01	-24.24 \pm 0.28
E92Q	-69.33 \pm 0.26	-40.18 \pm 0.16	86.52 \pm 0.30	-5.33 \pm 0.01	-25.32 \pm 0.33
E138A	-71.40 \pm 0.38	-40.18 \pm 0.16	88.81 \pm 0.31	-5.33 \pm 0.00	-28.10 \pm 0.32
E138K	-51.23 \pm 0.28	-66.06 \pm 0.14	95.14 \pm 0.45	-5.09 \pm 0.02	-27.24 \pm 0.33
G140C	-68.24 \pm 0.27	-31.23 \pm 0.21	77.24 \pm 0.38	-6.13 \pm 0.00	-28.36 \pm 0.41
G140S	-72.13 \pm 0.25	-35.26 \pm 0.15	84.61 \pm 0.25	-5.31 \pm 0.03	-28.09 \pm 0.38
Y143C	-56.27 \pm 0.24	-58.53 \pm 0.18	92.68 \pm 0.37	-5.21 \pm 0.01	-27.33 \pm 0.35
Y143H	-63.26 \pm 0.30	-48.18 \pm 0.17	89.22 \pm 0.26	-5.44 \pm 0.02	-27.66 \pm 0.29
Y143R	-82.50 \pm 0.32	-24.98 \pm 0.31	85.76 \pm 0.26	-5.48 \pm 0.01	-27.20 \pm 0.27
S147G	-57.25 \pm 0.41	-62.81 \pm 0.17	97.35 \pm 0.41	-4.30 \pm 0.02	-27.01 \pm 0.32
Q148H	-68.33 \pm 0.25	-39.20 \pm 0.16	87.29 \pm 0.40	-6.00 \pm 0.02	-26.24 \pm 0.28
Q148K	-80.59 \pm 0.25	-29.98 \pm 0.22	93.61 \pm 0.32	-5.24 \pm 0.01	-22.20 \pm 0.30
Q148R	-58.32 \pm 0.29	-63.06 \pm 0.14	103.06 \pm 0.23	-4.05 \pm 0.01	-22.37 \pm 0.24
N155H	-66.21 \pm 0.38	-42.43 \pm 0.17	88.97 \pm 0.31	-6.02 \pm 0.03	-25.69 \pm 0.27

All units are kcal/mol.

Table S6. The detail energy components contribution of calculated binding free energies of DTG binding to mutated HIV-1 IN.

Mutations	ΔE_{ele}	ΔE_{vdw}	$\Delta G_{\text{pol,PB}}$	$\Delta G_{\text{nonpol,PB}}$	$\Delta G_{\text{total,PB}}$
WT	-82.87 \pm 0.41	-35.67 \pm 0.18	90.95 \pm 0.34	-5.24 \pm 0.02	-32.83 \pm 0.31
T66A	-82.33 \pm 0.39	-33.01 \pm 0.22	87.39 \pm 0.28	-4.58 \pm 0.01	-32.53 \pm 0.39
T66I	-89.27 \pm 0.35	-38.14 \pm 0.21	99.68 \pm 0.41	-5.00 \pm 0.02	-32.73 \pm 0.40
T66K	-68.47 \pm 0.45	-59.21 \pm 0.29	99.76 \pm 0.36	-4.02 \pm 0.01	-31.97 \pm 0.42
E92Q	-73.20 \pm 0.33	-40.18 \pm 0.25	86.86 \pm 0.38	-6.30 \pm 0.02	-32.82 \pm 0.36
E138A	-75.89 \pm 0.42	-38.25 \pm 0.22	86.33 \pm 0.45	-5.01 \pm 0.03	-32.82 \pm 0.31
E138K	-65.32 \pm 0.40	-59.21 \pm 0.27	97.62 \pm 0.35	-5.12 \pm 0.03	-32.03 \pm 0.32
G140C	-80.82 \pm 0.40	-39.20 \pm 0.28	92.31 \pm 0.29	-5.04 \pm 0.00	-32.75 \pm 0.34
G140S	-85.50 \pm 0.41	-30.25 \pm 0.26	87.88 \pm 0.31	-4.31 \pm 0.00	-32.18 \pm 0.29
Y143C	-76.21 \pm 0.37	-30.32 \pm 0.24	79.40 \pm 0.31	-5.37 \pm 0.01	-32.50 \pm 0.43
Y143H	-81.68 \pm 0.43	-35.67 \pm 0.31	89.89 \pm 0.32	-4.96 \pm 0.02	-32.42 \pm 0.38
Y143R	-75.34 \pm 0.36	-32.74 \pm 0.23	80.88 \pm 0.33	-4.33 \pm 0.01	-31.53 \pm 0.46
S147G	-66.47 \pm 0.43	-58.21 \pm 0.19	97.45 \pm 0.41	-5.21 \pm 0.03	-32.44 \pm 0.37
Q148H	-88.61 \pm 0.47	-34.95 \pm 0.24	96.68 \pm 0.52	-4.89 \pm 0.01	-32.77 \pm 0.32
Q148K	-81.64 \pm 0.35	-38.77 \pm 0.18	92.50 \pm 0.36	-4.62 \pm 0.01	-32.53 \pm 0.33
Q148R	-72.13 \pm 0.44	-36.35 \pm 0.32	81.14 \pm 4.25	-5.24 \pm 0.02	-32.58 \pm 0.28
N155H	-63.89 \pm 0.32	-49.77 \pm 0.33	87.54 \pm 4.25	-6.31 \pm 0.02	-32.43 \pm 0.40

All units are kcal/mol.

Table S7. The computational alanine-scanning mutagenesis results for HIV-1 IN-JMC6F and RNase H-JMC6F.

Energy	HIV-1 IN								HIV-1 RNase H				
	D64A	T66A	L68A	D116A	T143A	Q148A	E152A	K159A	D443A	E478A	W535A	K540A	D549A
$\Delta\Delta E_{\text{ele}}^a$	-3.56	1.91	0.01	-9.50	-0.29	-4.94	-16.12	3.04	-4.87	0.16	-4.57	-9.76	-14.10
$\Delta\Delta E_{\text{vdw}}^b$	0.36	1.73	0.75	0.68	1.60	0.53	0.71	0.08	0.50	0.73	3.10	0.12	0.92
$\Delta\Delta G_{\text{pol-PB}}^c$	19.37	-0.50	-0.08	20.43	-0.81	6.83	19.89	-2.22	47.93	13.35	-2.72	4.62	13.99
$\Delta\Delta G_{\text{nonpol-PB}}^d$	-0.04	0.03	0.07	-0.01	0.31	0.02	-0.03	0.00	-0.03	-0.01	0.27	0.00	0.02
$\Delta\Delta G_{\text{CAS}}^e$	16.13	3.17	0.65	11.58	0.79	2.43	4.45	0.90	34.30	9.50	0.51	-0.04	5.17

^{a-e} $\Delta\Delta = \Delta_{\text{MUT}} - \Delta_{\text{WT}}$. All units are kcal/mol.

Table S8 The detail energy components contribution of calculated binding free energies of JMC6F binding to mutated HIV-1 IN.

Mutation	ΔE_{ele}	ΔE_{vdw}	$\Delta G_{\text{pol,PB}}$	$\Delta G_{\text{nonpol,PB}}$	$\Delta G_{\text{total,PB}}$	$\Delta\Delta G_{\text{calc}}^{\text{a}}$
WT	-78.21 \pm 0.45	-25.18 \pm 0.17	86.32 \pm 0.34	-4.83 \pm 0.01	-21.89 \pm 0.27	0.00
T66A	-65.02 \pm 0.27	-29.19 \pm 0.13	77.46 \pm 0.29	-5.13 \pm 0.01	-21.88 \pm 0.20	0.01
T66I	-71.06 \pm 0.34	-24.82 \pm 0.15	79.11 \pm 0.33	-4.84 \pm 0.03	-21.61 \pm 0.15	0.28
T66K	-71.25 \pm 0.28	-27.01 \pm 0.15	83.58 \pm 0.21	-4.79 \pm 0.01	-19.47 \pm 0.20	0.14
E92Q	-70.84 \pm 0.28	-28.11 \pm 0.16	82.27 \pm 0.25	-4.96 \pm 0.02	-21.64 \pm 0.19	0.25
E138A	-79.47 \pm 0.41	-31.58 \pm 0.18	90.38 \pm 0.23	-5.17 \pm 0.01	-25.85 \pm 0.20	-0.78
E138K	-88.64 \pm 0.52	-21.77 \pm 0.18	93.32 \pm 0.36	-4.33 \pm 0.03	-21.41 \pm 0.23	0.48
G140C	-80.11 \pm 0.31	-22.33 \pm 0.15	83.79 \pm 0.25	-4.18 \pm 0.01	-22.83 \pm 0.20	-1.23
G140S	-80.78 \pm 0.29	-22.02 \pm 0.19	78.59 \pm 0.21	-4.60 \pm 0.01	-28.81 \pm 0.19	-0.88
Y143R	-65.60 \pm 0.51	-25.03 \pm 0.16	73.50 \pm 0.40	-4.67 \pm 0.02	-21.81 \pm 0.19	0.76
Y143C	-73.57 \pm 0.34	-25.11 \pm 0.15	83.29 \pm 0.28	-4.74 \pm 0.01	-20.13 \pm 0.18	-0.16
Y143H	-66.60 \pm 0.31	-26.94 \pm 0.17	76.58 \pm 0.25	-5.10 \pm 0.02	-22.05 \pm 0.15	0.08
S147G	-73.82 \pm 0.34	-26.93 \pm 0.15	85.19 \pm 0.31	-4.93 \pm 0.00	-20.49 \pm 0.19	0.40
Q148H	-64.67 \pm 0.32	-36.41 \pm 0.18	82.37 \pm 0.27	-5.65 \pm 0.01	-24.37 \pm 0.22	-2.48
Q148K	-85.33 \pm 0.28	-32.34 \pm 0.14	92.79 \pm 0.16	-4.95 \pm 0.00	-29.83 \pm 0.17	-3.13
Q148R	-78.85 \pm 0.30	-25.84 \pm 0.16	88.57 \pm 0.30	-4.86 \pm 0.02	-20.98 \pm 0.84	0.91
N155H	-77.37 \pm 0.33	-27.34 \pm 0.15	87.96 \pm 0.32	-4.93 \pm 0.01	-21.68 \pm 0.22	2.10

^aCalculated binding free energy by MM/PBSA method in this work. $\Delta\Delta G_{\text{calc}}$ is defined as the change of binding free energy using WT as a reference.

All units are kcal/mol.

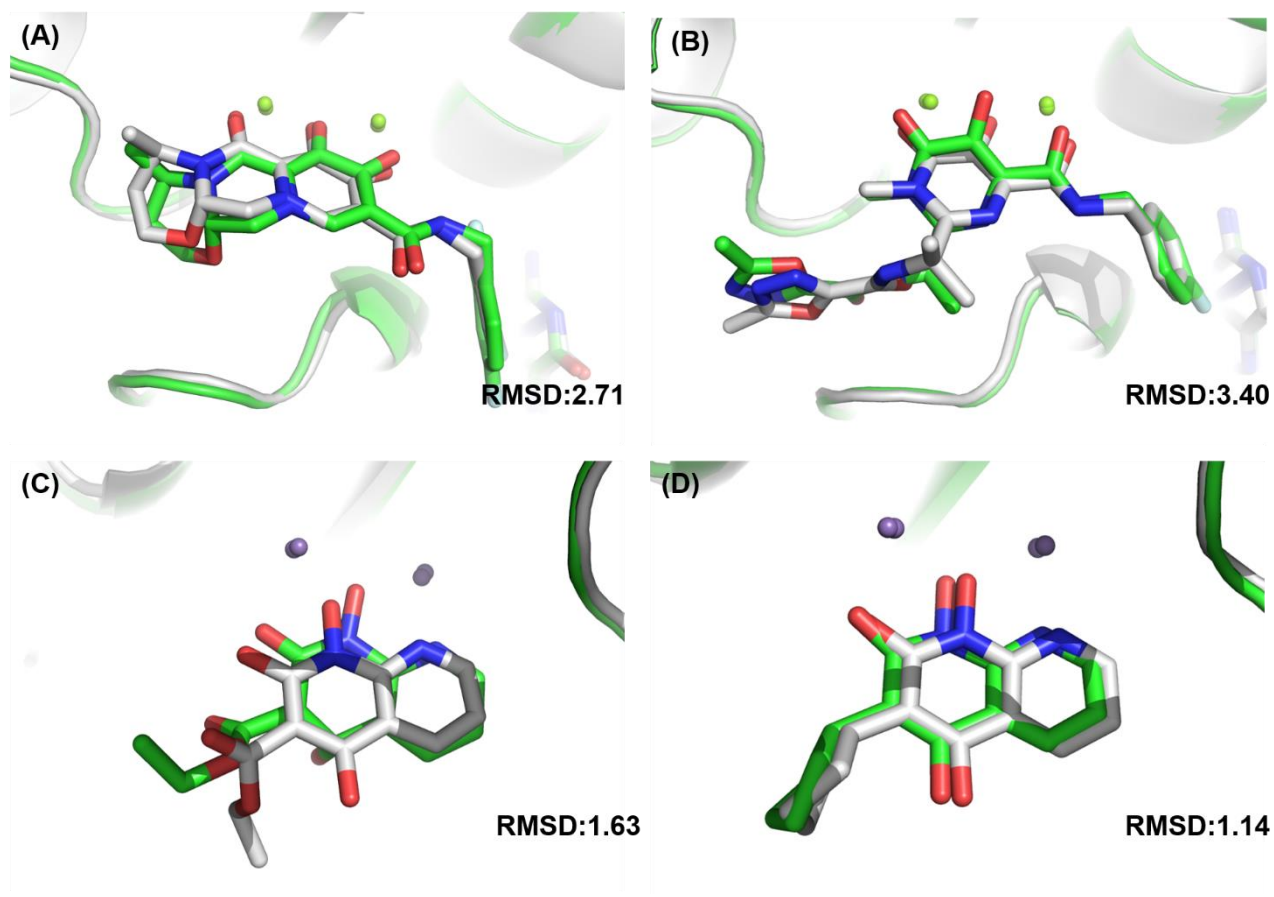


Fig S1. Structural superimposition of the cross-docking poses (green) and the corresponding co-crystal pose (white) of DTG (A), RAL (B), MK1 (C) and MK2 (D) binding with HIV-1 IN and RT.

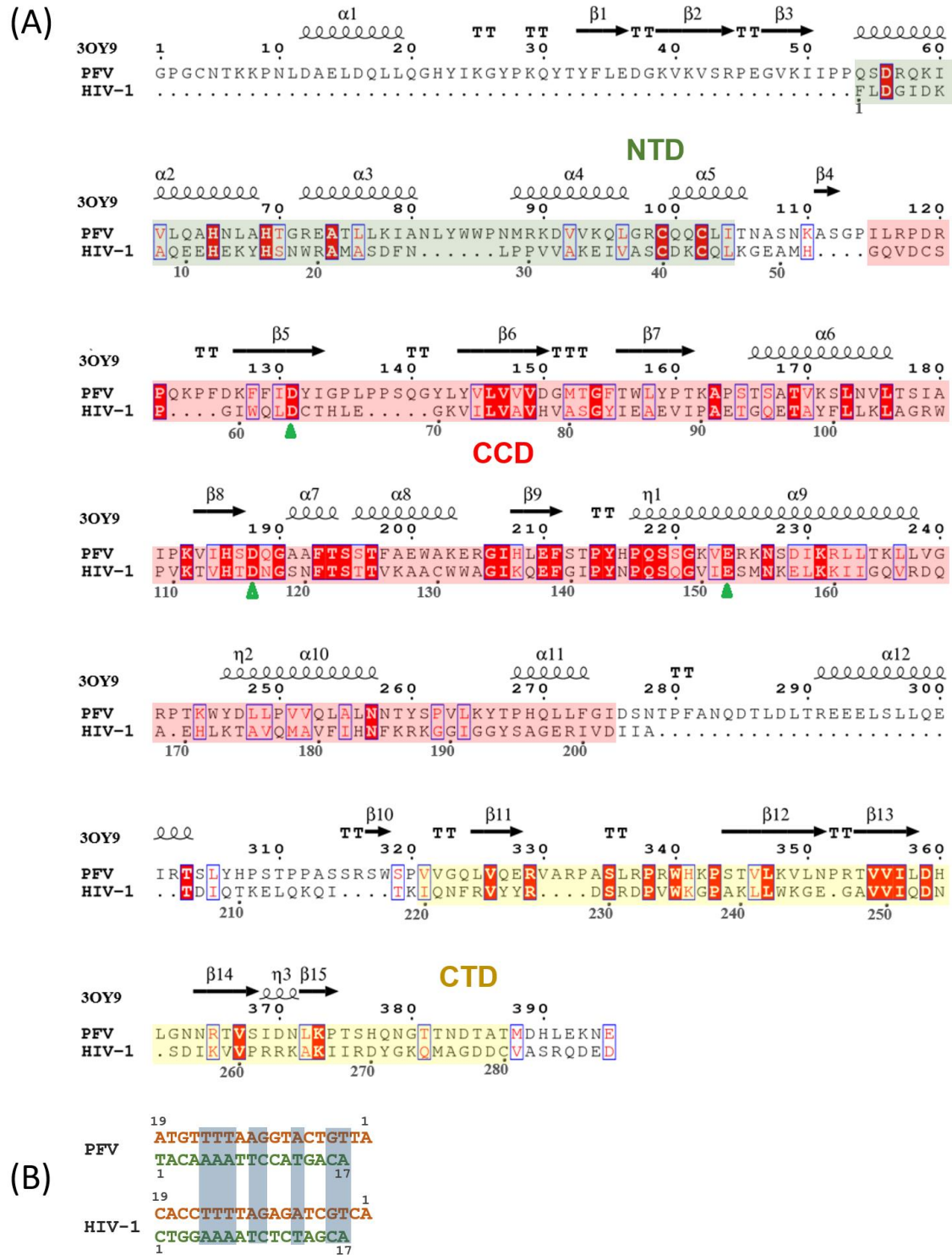


Fig S2. PFV and HIV-1 IN sequence alignment. (A) The structure-based sequence alignment of PFV/HIV-1 integrase. The CTD, CCD and NTD domains are shaded in yellow, red, green, respectively. Key residues involved in DDE motifs of CCD are indicated by green filled triangles. (B) The sequence alignment of PFV/HIV-1 viral U5 DNA end sequences. The nontransferred and reactive strands are colored orange and green, respectively. The conserved regions were highlighted in blue background.

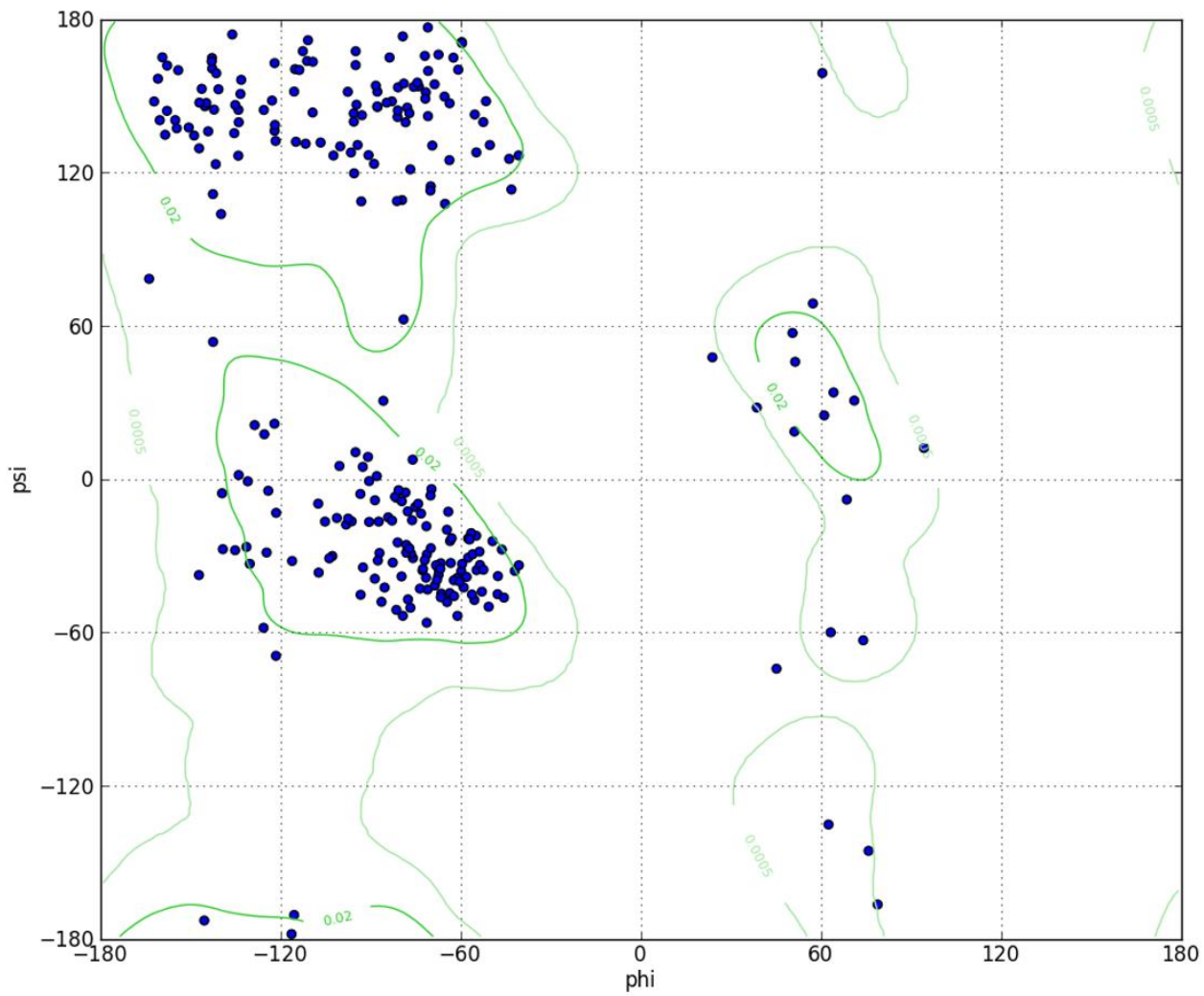


Fig S3. Ramachandran plot of the HIV-1 IN homology model.

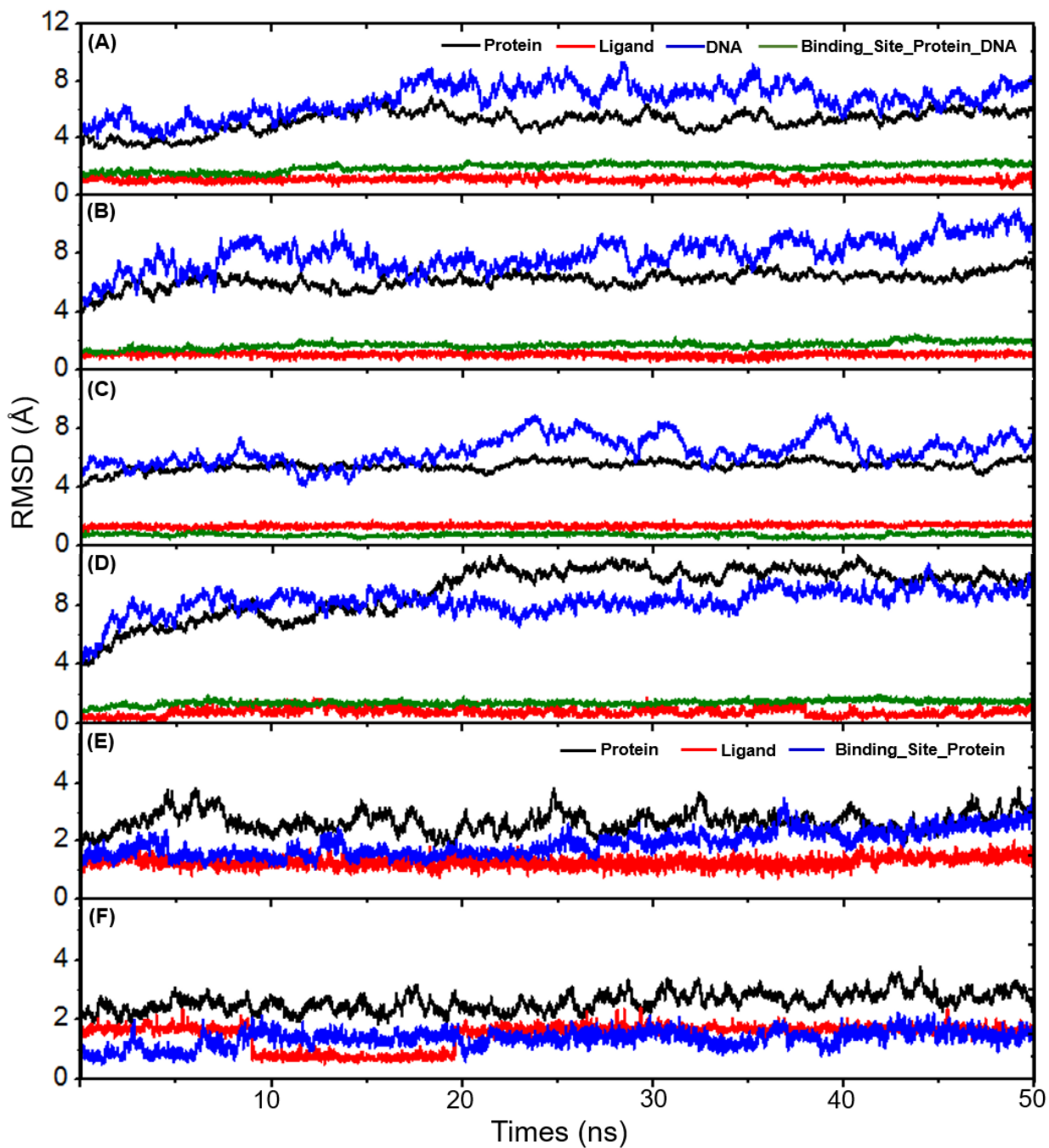


Fig S4. The monitored root mean squared deviation (RMSD) of the six wide type MD simulation system: (A) IN-JMC6F, (B) IN-DTG, (C) IN-E, (D) IN-RAL, (E) RT-JMC6F and (F) RT-MK1.

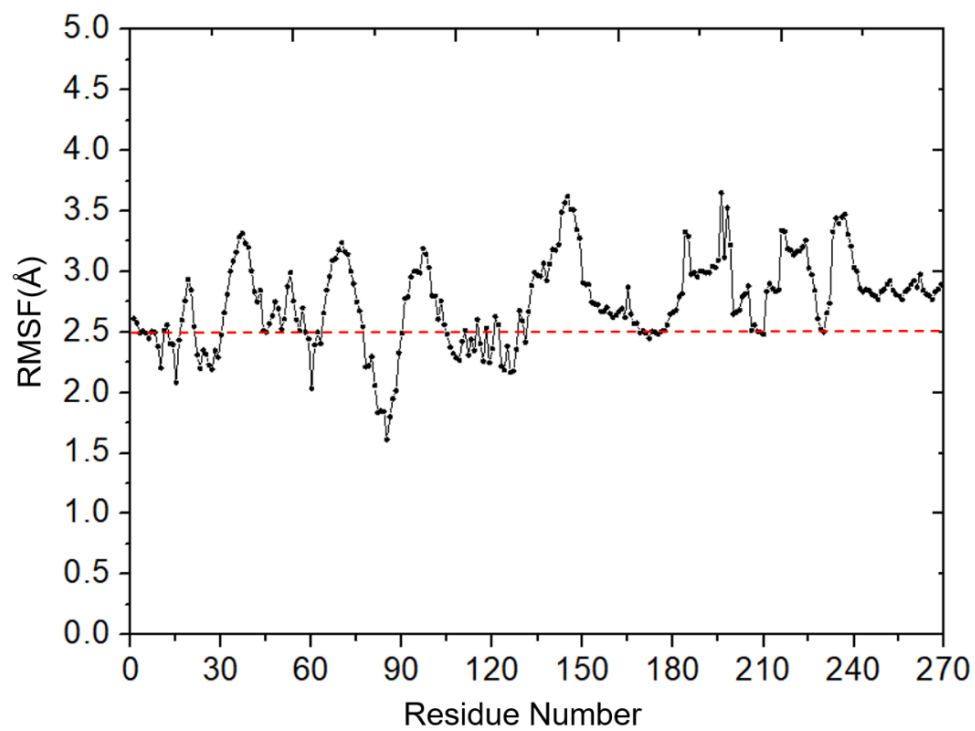


Fig S5. RMSF of the HIV-1 integrase in the simulation trajectory of JMC6F-IN system.

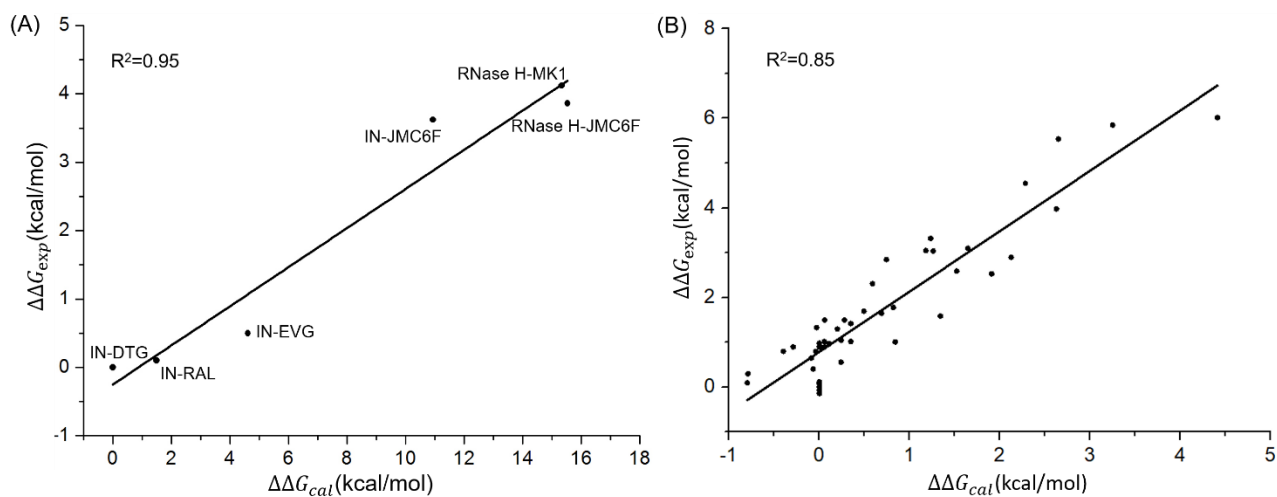


Fig S6. Correlation between the binding energy difference $\Delta\Delta G$ of (A) inhibitors binding with wide type HIV-1 IN and RNase H calculated in this work and that estimated binding energy based on experiments values. (B) of RAL, EVG and DTG binding with wide type and mutant type HIV-1 IN calculated in this work and that estimated on experiments.

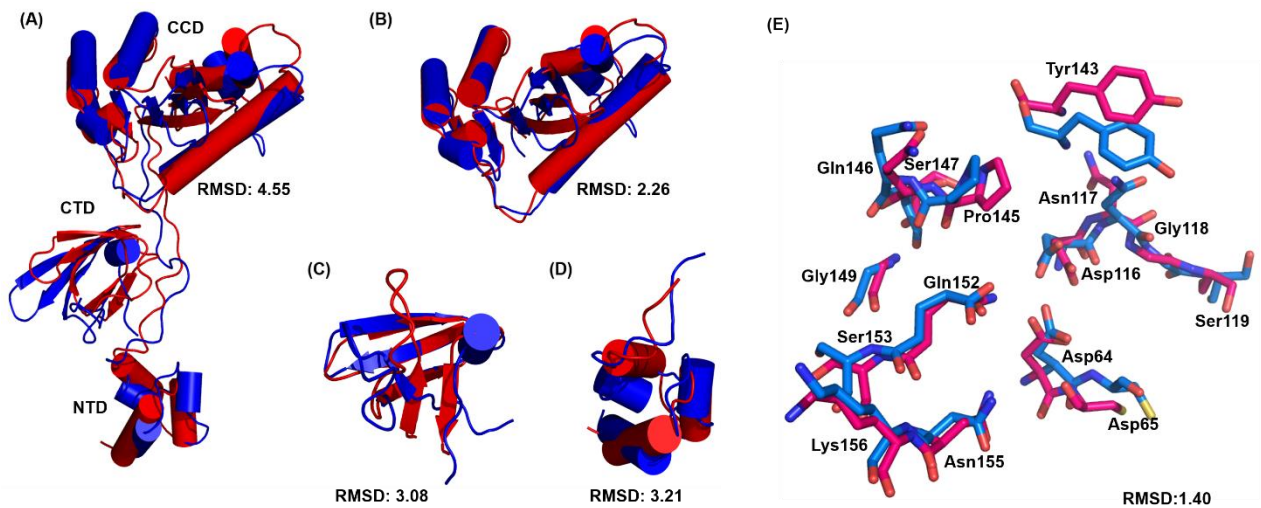


Fig S7. Superimposition of cryo-EM structure of HIV-1 integrase (PDB ID: 5U1C[89]) and the the constructed model. (A) the whole HIV-1 IN proteins. (B) CCD regions. (C) CTD regions. (D) NTD regions(E) Residues of binding site. Helices were depicted as cylinders, β -sheets as arrows, random-coil as tube, and residues of binding site were shown as sticks. Cryo-EM structure and the constructed model were colored in red and green, respectively. The RMSDs between the homology model and cryo-EM structure were also labeled, respectively.

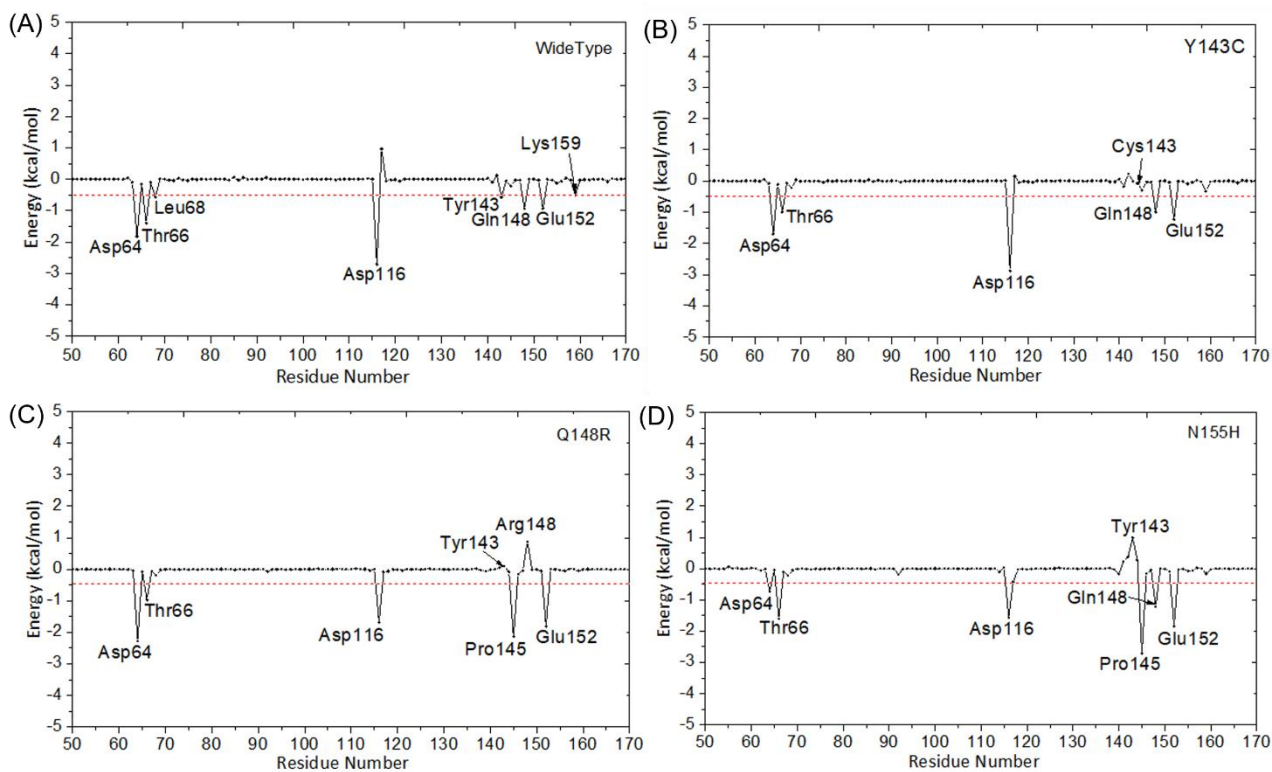


Fig S8. Intermolecular ligand receptor (per-residue) interaction spectrum of the (A) wide-type and mutant type (B) Y143C, (C) Q148R and (D) N155H intasome-JMC6F complex according to the MM-PBSA method. The residues with energy contribution more than 0.5 kcal/mol were labeled.

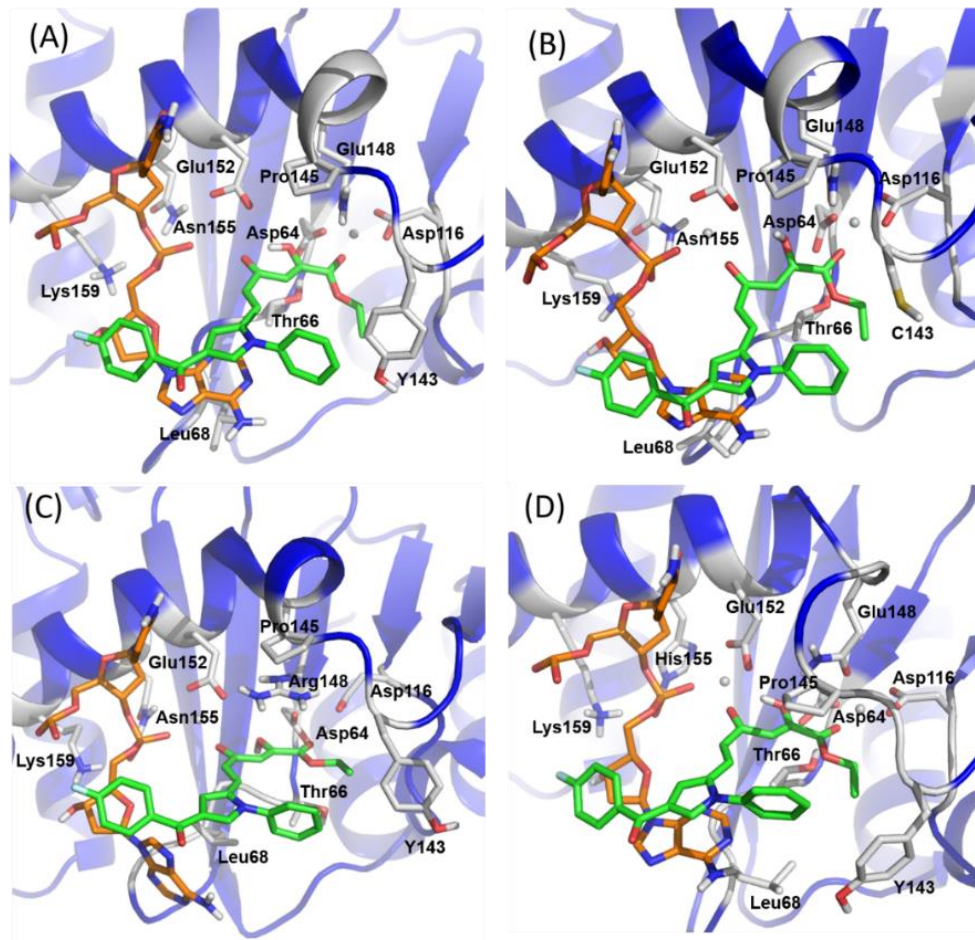


Fig S9. The MD-simulated structures of JMC6F in the (A) wide type, (B) Y143C, (C) Q148R and (D) N155H. IN is represented as blue cartoon. White stick representations are shown for IN residues in the intasome active site. Orange sticks represent nucleotides in the intasome active site. JMC6F is also shown as green sticks representation.